Journal of Soft Computing in Civil Engineering 2-2 (2018) 31-55

Contents lists available at SCCE

Journal of Soft Computing in Civil Engineering

Journal homepage: www.jsoftcivil.com

Profiled Composite Slab Strength Determination Method

K. Mohammed[1], I.A. Karim[2], F.N.A.A. Aziz[3], T.H. Law[3]

1. Senior Lecturer, Department of Civil & Water Resources Engineering, University of Maiduguri, Maiduguri, Nigeria
2. Senior Lecturer, Department of Civil Engineering, University Putra Malaysia, Serdang, Malaysia
3. Associate Professor, Department of Civil Engineering, University Putra Malaysia, Malaysia

Corresponding author: *engrkachalla@unimaid.edu.ng*

https://doi.org/10.22115/SCCE.2018.102399.1030

ARTICLE INFO

Article history:
Received: 27 October 2017
Revised:
Accepted: 05 February 2018

Keywords:
Slope-intercept method;
Reliability;
Profiled composite slab;
Longitudinal shear;
First order reliability method;
Strength test.

ABSTRACT

The purpose of this article is to develop a new numerical approach for determining the strength capacity of a profiled composite slab (PCS) devoid of the current challenges of expensive and complex laboratory procedure required for establishing its longitudinal shear capacity. The new Failure Test Load (FTL) methodology is from a reliability-based evaluation of PCS load capacity design with longitudinal shear estimation under slope-intercept (m-k) method. The limit-state capacity development is through consideration of the experimental FTL value as the maximum material strength, and design load equivalent estimation using the shear capacity computation. This facilitates the complex strength verification of PDCS in a more simplified form that is capable of predicting FTL value, which will aid in determining the longitudinal shear of the profiled deck composite slab with ease. The developed strength determination effectively performs well in mimicking the probabilistic deck performance and composite slab strength determination. The strength test performance between the developed scheme and the experiment-based test results indicates high similarity, demonstrating the viability of the proposed strength determination methodology.

How to cite this article: Mohammed K, Karim IA, Aziz FNAA, Law TH. Profiled composite slab strength determination method. J Soft Comput Civ Eng 2018;2(2):31–55. https://doi.org/10.22115/scce.2018.102399.1030

1. Introduction

Composite action between the profiled sheeting deck and the hardened concrete that comes into play with effective development of longitudinal shear at the steel-concrete interface give birth to a popular construction method known as profiled composite slab (PCS)construction. However, despite the numerous advantages associated with using PCS in the construction industry, costlier and time-consuming laboratory procedures accounts for its shear characterization [1]. Moreover, this applies to all the known methods for the determination of its shear bond capacity. Longitudinal shear capacity defines the ultimate strength of profiled composite slab [2]. However, several factors are known to influence the longitudinal shear capacity of a PCS, and that hinders the development of a simplified PCS strength determination [3,4]**.** There is a serious need to address this drawback. Hence, this paper attempts to develop a longitudinal shear-based numerical strength determination model for the PCS that considers the randomness associated with its strength influencing factors.

2. Literature review

The quest for replacing the uneconomical and complex strength verification of composite slab led to both several numerical and experimental approach studies [5,6]. Abdullah and Samuel Easterling [5] and Abdullah, Kueh [6]studies result yields the developments of proposals for PCS shear capacity modeling that takes in to account the slab slenderness function. Abdullah and Samuel Easterling [5] study experiment similarly show the determination of shear bond-end slip behavior of composite slab through force equilibrium method. The author's finite element model of the slab fails to yield positive result due to modeling limitation because of the strength influencing factors. Similarly, Abdullah, Kueh [6] study finding also reveals the slab slenderness function influence on the longitudinal shear bond. The authors have presented the result of linear interpolation of shear bond that includes the effect of the slenderness and concludes to have performed satisfactorily in the prediction of the composite slab capacity.

In another PCS study, it shows the simulation results for long slab specimens reflect true resembles of the slab performance in comparisons with experimental literature findings with the exception of few where the comparative behavioral analysis for the short span shows behavioral variations between the model result and experiments [7,8]. Critics of the FE analysis application for shear bond capacity for composite slab shows that shear bond is geometry dependent, and this signifies the need to carry out a full-scale test on PCS to be utilized in the FE formulations. Hence, FE modeling will become uneconomical since the test has to be conducted by utilizing the data [5]. Therefore, in order to augment this drawback, there is a need to use a different numerical approach in finding a solution to a simplified PCS strength determination, and the reliability method is one good option other than finite element approach. Hence, this paper focuses on using the reliability method in exploring its potentials to curb conservatism in design and strength verification of PCS.

Reliability method studies on the performance of composite slab are few because very little areas are covered [9]. The few areas covered are found in the literature [1]. There are numbers of methods that are useful in determining the strength parameter, for example, the *m-k* and partial interaction methods. This study uses slope-intercept (*m-k*) method for the determination of the PCS longitudinal shear resistance parameter.

3. Methodology

The *m* and *k* parameters are obtained after conducting experimental flexural testing of the composite slab specimens, and deducing from the linear relationship plots of vertical shear, V_t / bd_p against the shear bond, A_p / bl_s for two groups of test values of long, *X* and short, *Y* specimens, as depicted in Fig. 1. The standard full-scale laboratory testing procedure for the two test groups requires a minimum of three test specimens for each long and short shear specimens as shown in Fig. 1.

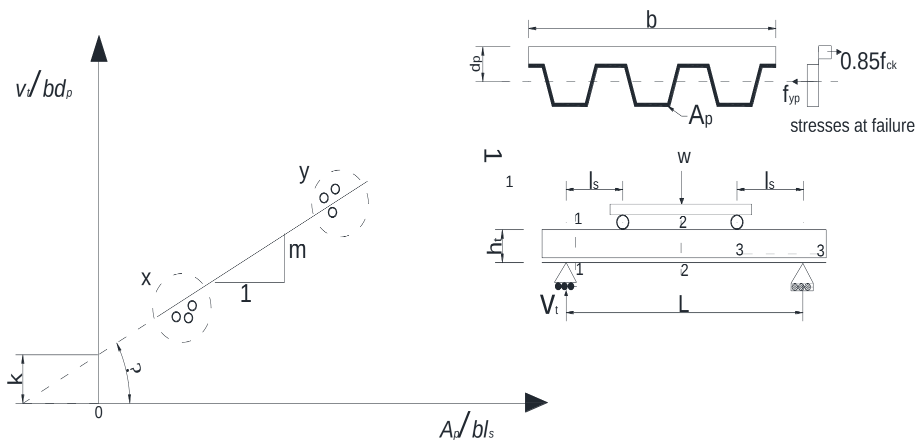

Fig. 1. Typical slope-intercept method laboratory setup [10].

In Fig. 1, A_p stands for the metal deck effective cross-sectional area and f_{yp} represents its yield strength value. Similarly, the centroids distance is d_p, and l_s is the shear span length (normally taken as $L / 4$, where L is the clear span between supports) [11]. For ductile failure condition, the support reaction is computed using Eq. (1).

$$V_t = w / 2 \tag{1}$$

However, in cases where it exhibits a brittle failure condition, a factor of 0.8 [12] is applied to Eq. (1). The ratio l_s / d_p "herein referred to as inverted slenderness in this paper" plays a critical role in defining PCS strength capacity. Hence, the vertical shear stress, V_t / bd_p for composite slab at equilibrium is

$$\frac{V_t}{bd_p} = \frac{m}{bd_p l_s} . \frac{A_p f_{yp}}{bl_s} \tag{2}$$

Johnson [11] study finding reveals that f_{yp} has insignificant influence on longitudinal shear computation. Hence Eq. (2) reduces to Eq. (3).

$$\frac{V_t}{bd_p} = m(\frac{A_p}{bl_s}) + k = \tau_{u,rd} \tag{3}$$

The parameters *m* and *k* in Eq. (3) are defined previously, and are determined from full-scale laboratory procedure as shown in Fig. 1. The V_t value for a slab width, $b \leq$ design shear resistance, $V_{i,Rd}$ the semi-empirical expression in Eq. (4) is the PCS design shear resistance function.

$$V_{i,Rd} = \frac{bd_p}{\psi}[m(\frac{A_p}{bl_s}) + k] \tag{4}$$

The shear connection factor ψ had a value of 1.25 [13].

3.1. Failure testing loads

This study uses full-scale experimental laboratory tests results conducted by several authors [3,14–16] serves as input variables for the failure test load (*FTL*) in developing the PCS performance function. Marimuthu, Seetharaman [14] conducted an experimental evaluation of PCS in accordance to the EC4 standard using M20 grade concrete. The testing shear span lengths l_s are 320 mm, 350 mm, 380 mm and 850 mm, 950 mm, 1150 mm. Similarly, Hedaoo, Gupta [16] also carried conducted its experimental testing with Colour Roof India deck span that has A_p value of 839 mm^2. The author slab specimen (3 m length) has a nominal depth of 102 mm, width, b of 830 mm, concrete thickness above the flange, h_c and d_p values of 50 mm and 76.77 mm, respectively. Due to temperature and shrinkage effect control, the author placed 6 mm Φ mesh at mid concrete depth of 25 mm from the top surface, and similarly conducted the testing in accordance with EC4 [17] provisions under varying l_s values of 300 mm, 375 mm, 450 mm, 525 mm, 600 mm and 675 mm.

Furthermore, Cifuentes and Medina [3] conducted its experiments using two different galvanized trapezoidal sheeting desk, MT-60 (AW specimens) and MT100 (BT specimens) with respective A_p values of 1003 mm^2 and 1032 mm^2, and performed the experimental testing procedure according to EC4 standard. The author uses two shear span lengths both for AW specimen (0.575 m and 1.0 m) and BT specimens (0.75 m and 1.0 m) with each shear span length having three short and long specimens designated by the third letter in the slab type (Table 1). However, d_p value varies for both short (103 mm, 123 mm) and long specimens (143 mm, 193 mm) under both AW and BT specimens. Similarly, Holmes, Dunne [15] uses Conflor 60 steel deck profiled for the experimental composite shear capacity testing with characteristics A_p value of 765.6 mm^2, f_{yp} of 350 N/mm^2, and d_p of 100.4 mm.

However, the authors' performed the experimental testing in accordance with the EC4 specification, and fitted the slab with 19 mm shear studs, at a value of 450 mm and 900 mm, respectively, but could not conduct the cyclic loading test as required by the EC4 provision. The author's reason for not conducting the cyclic test is based on literature findings that reveal that cyclic loading has insignificant influence on the load carrying capacity of composite slab [14].

Table 1
Longitudinal shear strength parameters from a different experiment.

source	Label	l_s ***mm***	FTL ***kN***		$\tau_{u,rd}$ ***N/mm***^{2}	***N/mm***^{2}	
						m	k
Marimuthu, Seetharaman [14]	1	320	55.625		0.281	87.956	0.003
	2	350	52.191		0.285		
	3	380	47.340		0.241		
	4	850	22.612		0.122		
	5	950	26.920		0.112		
	6	1150	16.391		0.097		
Cifuentes and Medina [3]	AWS-1	575	45.79	AV. 45.86	0.240[1]	75.026	0.099
	AWS-2	575	46.44				
	AWS-3	575	45.35				
	AWL-1	1000	47.69	AV. 47.82	0.180[a]		
	AWL-2	1000	46.34				
	AWL-3	1000	49.44				
Hedaoo, Gupta [16]	1-3	300	54.301		0.322	81.95	0.046
	4-6	375	50.595		0.266		
	7-9	450	42.650		0.230		
	10-12	525	37.195		0.204		
	13-15	600	31.523		0.184		
	16-18	675	21.109		0.169		
Holmes, Dunne [15]	C450	450	86.75		0.712	197.14	0.1602
	C900	900	53.02		0.436		
Cifuentes and Medina [3]	BTS-1	750	58.70	AV. 59.68	0.409[a]	189.78	0.058
	BTS-2	750	60.58				
	BTS-3	750	59.77				
	BTL-1	1000	67.33	AV. 65.76	0.321[a]		
	BTL-2	1000	65.56				
	BTL-3	1000	64.38				

[a] This value are recomputed from the original data source

Table 1 shows the PCS properties including the *FTL* values and their respective shear strength parameters from several full-scale laboratory-testing procedures by different authors. However, a suspected computational errors in the values of A_p/bl_s in Cifuentes and Medina [3] makes it necessary in re-computing the A_p/bl_s values in order to obtain the correct *m* and *k* parameters (Fig. 2). For example in the experiment [3], the AW specimens which has a uniform A_p and b values of 1003 mm^2 and 927 mm, respectively, and 575 mm, 1.0 m as l_s for both short and long specimens should have uniform values of A_p/bl_s in both short and long specimens sections; 0.001882 and 0.001082 instead of 0.001793 and 0.001031 values found in the literature. Hence, the values are recomputed to obtain the *m* and *k* parameters as 189.78, 0.058 N/mm^2 and 75.02, 0.10 N/mm^2 for the BT and AW specimens, respectively.

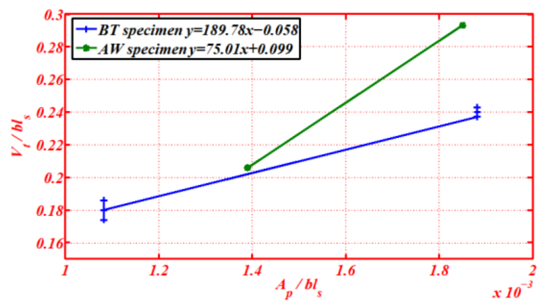

Fig. 2. *m* and *k* parameters determination for *AW* and *BT* slabs.

3.2. Reliability analysis

Structural components reliability is by reliability index or safety index, β value and its relationship with the failure probability is by the expression in Eq.(5) [9,18].

$$p_f = \Phi(\text{safety index value}) \tag{5}$$

Where Φ is the inverse of the standardized distribution function. For more details on this formulation, there are numbers of available good literatures [1]. Hence, **Fig. 3** depicts the reliability analysis syntax for a profiled deck composite slab that places focus on the material load carrying capacity and design load estimation from the shear resistance of composite slab under the *m-k* method. The maximum *FTL* values (in Table 1) represent the ultimate strength resistance of the material, and the design load computation is of the longitudinal shear strength capacity of the profiled deck composite slab. Therefore, accounting for the random variability, the PCS mean resistance, Q_m is [19,20]

$$Q_m = Q_n(M_n F_n P_n) \tag{6}$$

where Q_n is the nominal resistance, and has a bias factor of 1.0. Similarly, M_n, F_n, P_n are factors for material fabrication, mean ratio for component geometry and dimension, and professional factor for approximation, respectively. These factors mean resistance coefficient of variation, V_Q is from the expression in Eq. (7).

$$V_Q = \sqrt{(v_m^2 v_f^2 v_p^2)} \tag{7}$$

The parameters, v_m, v_f and v_p are the equivalent corresponding coefficient of variation, *COV* for the factors M_n, F_n, and P_n respectively. Hence, the values for the mean *COV* for these factors are 1.10, 0.1; 1.0, 0.05 and 1.11, 0.09, and are all normally distributed [9]. Consequently, this study V_Q value is 0.14 from the use of the expression in Eq. (7). Ellingwood and Galambos [21] characterizations are applied to get the *COV* value and distribution type for the parameters b and l_s as 0.17 and the lognormal distribution. (each with unit bias factor).

Hence, this study limit state is as shown by the expression in Eq. (8).

$$Q_m - \frac{2V_{i,Rd}}{L} = R - Q \tag{8}$$

The parameters $V_{i,Rd}$ and Q_m are from the use of Eq. (4) and (6), respectively. Eq. (9) show the equivalent transformed function of the expression in Eq. (8), and three discrete variables, X(1-3); *FTL, b,* and l_s (see Fig. 3) were identified.

$$\begin{aligned} R &= [(1 - \% / 100)X(1)] / l \\ Q &= slope * ((A_p / (X(2) * X(3) + \text{int}ercept * 2 * X(2) * d_p / \\ &\quad (span * 1.25 * 10^3) \end{aligned} \tag{9}$$

4. Result and discussion

Fig. 4 presents the performance index of PCS where l_r represent the ratio of FTL and design load from the longitudinal shear capacity, and the symbol α stands for shear span length; for example, α_{320} indicates shear span length of 320 mm. Relating to the FTL value source, the ratios are shown with different graphs from Fig. 4. For example, the ratio of the Marimuthu, Seetharaman [14] experimental failure test value to the deterministically computed design load is shown in A, graphs B, C, and D for the respective ratios from Hedaoo, Gupta [16], Cifuentes and Medina [3] and Holmes, Dunne [15]. It is interesting to study the decking sheet cross-section variation influence by examining the 3% change in area from 1003 mm^2 to 1032 mm^2. Similarly, the four indents marks on each plot show the influence of the reduced FTL from full test load value down to 30% decrease in value. This action evaluates the influence of the present capacity reduction factor of 0.8 that is applied to the failure test load while computing the shear bond capacity of the profiled deck composite slab [14].

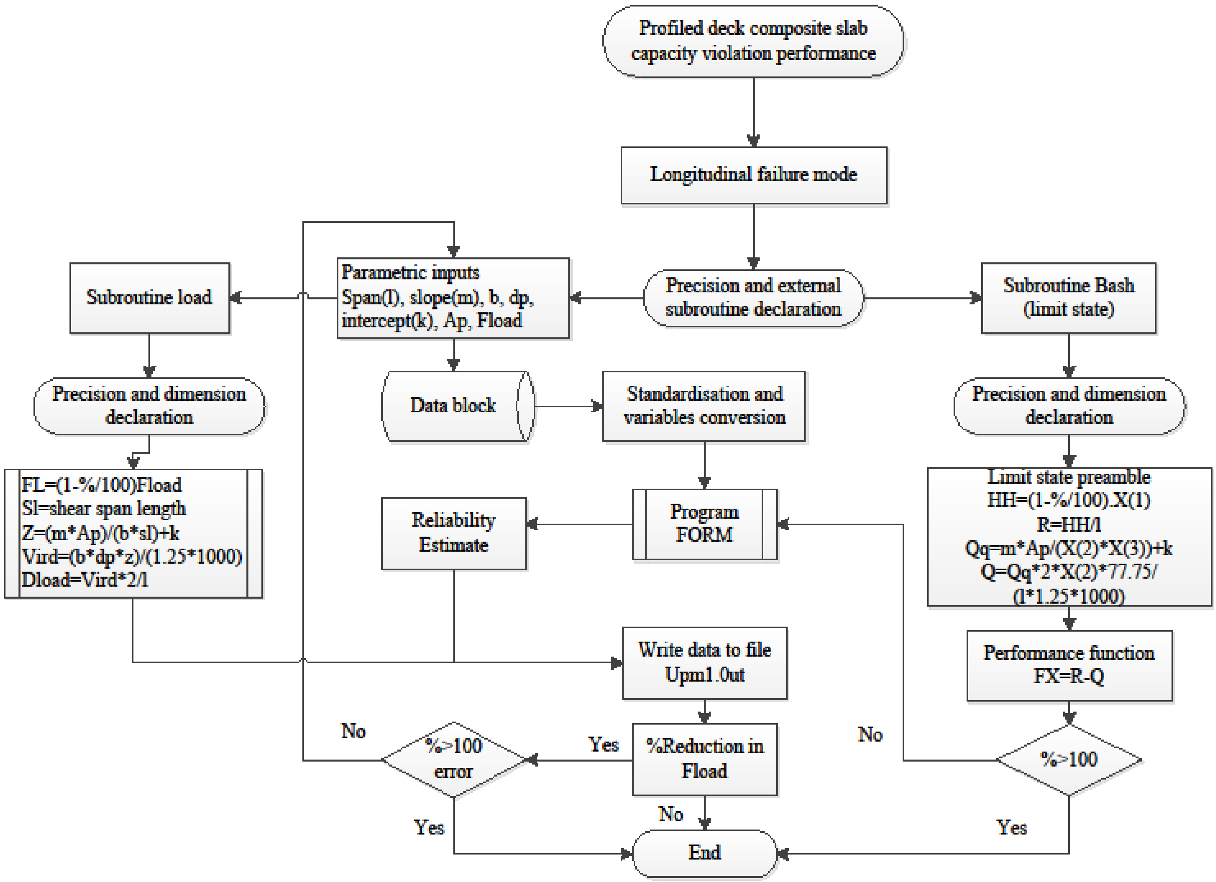

Fig. 3. Performance index determination flow.

As shown in Fig. 4, the result demonstrated a linear elastic relationship between l_r and β value. This behavior is not surprising because of the uniform strength value decrease. To establish the PCS load-carrying capacity, it is essential to relate its bearing capacity to the shear span length [22]. The peak and lowest points are the upper and lower tails for each α value as demonstrated in Fig. 4 that shows an increment in the safety indices value as the l_r value increases (the shorter the shear span length, the higher the safety value, and vice versa). For example, α_{1150} which has the lengthiest shear span length, has a lower safety value range. However, this may be due to the reported failure condition during the static and cyclic loading testing during the experiment. Interestingly, Fig. 4 (A and B) share similar characteristics, although in Fig. 4 (B), the α value ranges between 300 mm - 675 mm compared to 320 mm - 1150 mm range under Fig. 4 (A). Additionally, the lowest tail safety value for the safety is from the lengthiest. As illustrated previously, the behavior is because of the reported failure due to high slip value during the experimental tests for determining the strength load. Hedaoo, Gupta [16], reported the formation of flexural cracks which leads to a sudden drop in capacity accompanied by a 3.27 mm slip. The end slip value, considering the ductile behavior should not be more than 0.5 mm [4].

The failure of the major longer shear length specimen, either in the static or cyclic load test, happens when the shear span length is relatively close to the mid-span length of the test specimen. For example in Fig. 4 (B), the failed specimen has a span length of 2.7 m, and subtracting twice the α value results in moving the load position close to the mid-span. This action will definitely result in decreasing the load carrying capacity of the composite slab [16].

Decking cross section is a major strength-influencing factor for PCS, and its variation will significantly shows differences in the load carrying capacity. Adopting the use of a clear classification for the differential cross-section as illustrated in Fig. 4 (C), which takes into accounts both variations in cross section and shear span length. For example $\alpha_{575,A1}$ and $\alpha_{1000,A1}$ represent AW – slab specimens with the uniform cross-sectional area, and α values of 575 and 1000 mm, respectively. Hence, it is evident that the AW and BT slabs show similar result characteristics (Fig. 4 (C)), but the glaring difference in plot compactness compared to plots illustrated in Fig. 4 (A and B) is due to the variations in shear span lengths and decking sheet cross-section. The results also show that a 3% change in cross-sectional value of decking sheet will significantly influence the safety consideration of PCS. In contrast, Johnson [10] showed that a change in cross-section of about 24% from 1765 mm^2/m has no effect on the longitudinal shear strength, but the shear lengths under consideration were greater 1000 mm. However, the author similarly expresses that this might not be the case for a much smaller section. Chen [22] experimental study shows an increment of about 15.7% of vertical shear on a range of cross-sectional area similar to those reported previously before the contrasting argument. In that study experiment, though diameter 19 studs are used as the end anchorage, the test load capacity is greatly influenced by the shear studs. Hence, this section concludes that irrespective of the specimen cross section and span length, the safety value decreases with decreasing α value.

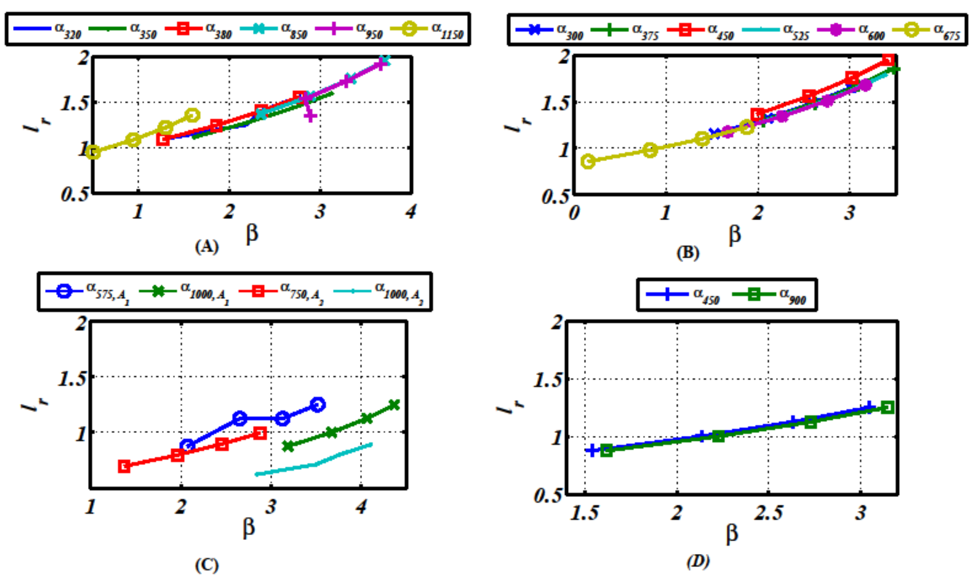

Fig. 4. Safety performances in relation to l_r value.

Cracks propagation triggers a longitudinal shear failure, and this will result in loss of bond between the composite medium that will lead to brittle failure. This brittle form of failure is penalized with 20% reduction in the design resistance. In appraising the penalized load bearing capacity, Fig. 4 (D) shows the reliability indices having an average safety value of 2.2, and is slightly lower than the 2.9 benchmark. The difference in safety value is because of the limited shear span length (α_{450} and α_{900}) considered in that experiment, which falls short of the standard testing requirement.

The other factor apart from the shear span length is the decking sheet characteristics. This study explores to find the longitudinal shear value behavior from the use of several decking sheets and Fig. 5 provides an insight. A horizontal shear bond value of 0.3 MPa is within the acceptable end-slip that exhibits a ductile behavior [5]. Intuitively, the scattered behavior characteristics illustrated in Fig. 5, which shows a varying safety values between 2 and 3. This behavior is due to the sheeting deck characteristics difference that includes the A_s, f_{yd} and thickness values which are known to influence the composite deck's horizontal shear capacity.

Moreover, the results are shown in Fig. 5 provide a guide in choosing upper and lower safety ranges in relation to l_r (see Fig. 8). This section concludes that there is a positive linear correlation between l_r and β, with shear span length as an indicator (see Fig. 8, $p > 0.05$). It is pertinent to note that the α values are those that were able to withstand both static and cyclic load testing. Generally, the relatively longer shear span length commonly fails because of the harmful effect of cyclic loading test [3].

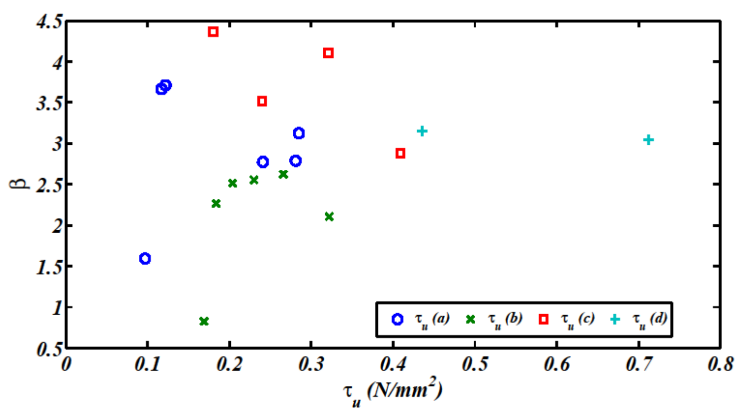

Fig. 5. Decking sheets characteristics influence the performance index of *PCS*.

4.1. Section slenderness effect

This study presents safety performance using the sectional inverted slenderness as explained in the previous section. The correct characterization of the PCS performance index significantly depends on that function. However, it is also important to take into consideration the differences in cross sections and yield strengths of the sheeting deck. Therefore, the inverted slenderness is multiplied with the decking sheet characteristics $A_p f_{yp}$. Hence, for simplicity the resulting product is a function. Fig. 6 shows the predicted performance from different penalized *FTL* considerations.

The slenderness value influence on PCS behavior is substantial [6]. The slenderness classification as found in the literature can be grouped as either slender (with low d_p / l_s value) or compact (with high d_p / l_s value) sections. The classification sounds rational, but a clear definitive boundary between the two still poses a serious challenge. Abdinasir, Abdullah [23] proposed a ratio of $1/7$ but heavily criticized because of the resulting consequences for slender section design using the result from compact slab testing can be potentially harmful in the practical sense. The performance depicted in Fig. 6 shows the decking strength diminishes from the compact region down to the slender case, and there is similar supportive behavior found in the literature [6]. All performance behavior in Fig. 6 exhibits near uniform trends for all the strength loads conditions with increased failure chances while the decreasing *FTL* values. This is understandable because the decreasing load capacity has little or no influence on the estimated design load from longitudinal shear capacity.

The two points in Fig. 6 that show a pronounced p_f value in relation to other established points are those that fail to withstand the cyclic loading test during laboratory strength testing as previously reported by the respective authors. The failed longer specimen had failure chances of 17.3 and 20.4% (see Fig. 6 at 80% *FTL*). Fig. 7 shows the relationship between the p_f and ϖ which is on the use of the 12 points that comprise six each of three long and three short test specimens from the two standard testing results. Fitting exponential trend gives the best fit, and it shows high correlation, as shown in Fig. 7. The behavior trend exhibited in that Figure is useful in formulating the numerical strength test function in this study. Hence, it is the conclusion of this section that decking strength diminishes from the compact region down to the slender section and decreasing *FTL* value show minimal influence on the design load estimation from the developed approach using the longitudinal shear capacity. Similarly, the use of exponential trend can suitably describe the failure performance estimation of PCS by the decking stiffness function that includes the cross-section and the slenderness parameter with high assurances.

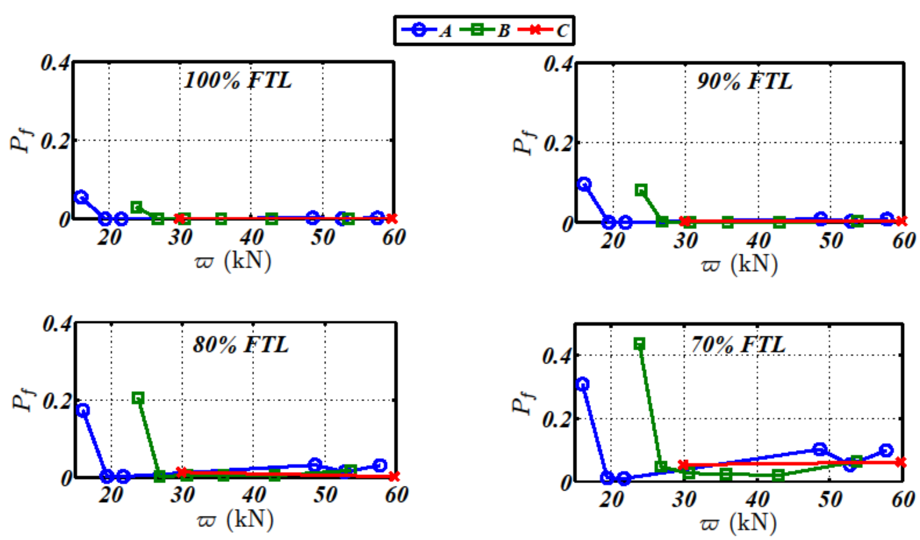

Fig. 6. Deck characteristics behavior influenced by penalized *FTL* values.

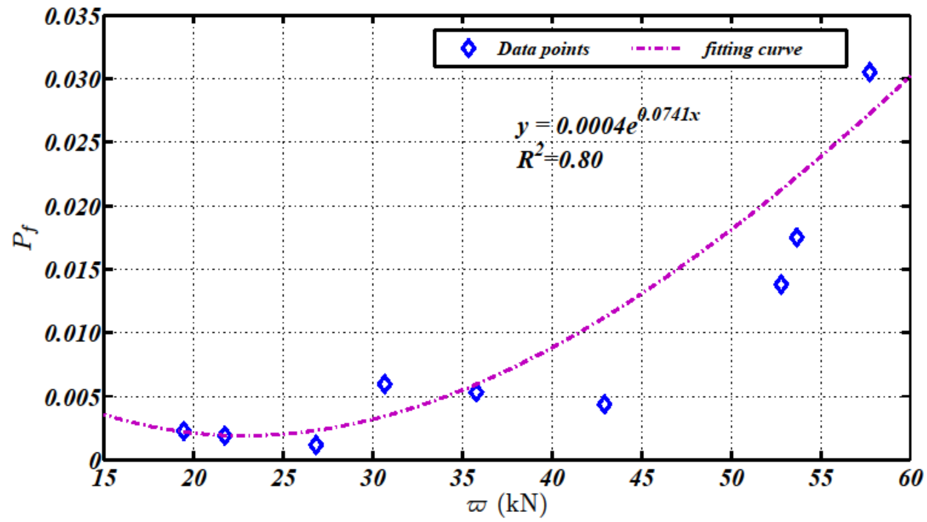

Fig. 7. Established relation between Deck characteristics behavior and failure probability at current EC4 [17] consideration for *FTL* in longitudinal strength parameter determination.

4.2. Load capacity model development

This section pulls together all the relevant findings from the previous section, with justifiable assumption where necessary in developing new *FTL* estimation function applicable under the *m-k* method. This new function will be devoid of the conservative experimental testing procedure that was mandatory for PCS strength verification.

Fig. 7, shows a high correlation between the performance function and established deck characteristics where the minimum and maximum experimental FTL values per span length are 5.464 kN, 18.542 kN and 7.036 kN, 18.1 kN from Marimuthu, Seetharaman [14] and [16], respectively. The l_s value is principally the determining factor in the adopted classification (compact and slender). Generally, $l/4$ can be used to determine l_s value theoretically [11]. However, the empirical assumption for l_s as $l/6$, though arguably, seems logical. If that is the case, the minima and maxima values will rightly fall into the $l/8$ and $l/6$ range. Therefore, since the values can be reasonably divided into two groups, the mean minimum, and maximum *FTL* values are 6.25 kN and 18.321 kN. Similarly, applying the same principle to obtain their corresponding mean design load values as 4.885 kN and 11.407 kN, respectively. These values are the average result of the minimum and maximum design load values of 4.03 kN, 11.853 kN and 5.74 kN, 10.96 kN. These values are taken for the whole full experimental testing result because of the shown ductile failure conditions. According to the study load ratio l_r defined; those values form 1.28 and 1.61 as the minimum and maximum l_r ratios.

Fig. 8 clearly shows the significance of l_r range with the fitted linear regressed line. The fitting is well suited because assuming equal variance in safety values between the regressed and the computed; the result shows no significant difference $(t = 0.086,\ dof = 22,\ p > 0.05)$. The choice of linear fitting suitably describes the actual data point behavior, though similar quadratic fittings yield nearly the same result. However, polynomials and cubic fittings give unfavorable conditions. Similarly, the policy for establishing a lower and upper safety index value of 1.94 and 2.85 by the minimum and maximum l_r values were defined previously (Fig. 8). These values are comparable with the 2.9 code specified value for irreversible flexural limit state violation. However, this latter value is generally shown to be uneven and verified by Honfi, Mårtensson [24].

In this study, no doubt the upper value is relatively close to the present target safety index of 2.9, though uneven. In statistics, the central tendency measure between sets of values is the mean value, μ. , and the evaluated lower and upper safety index is 2.4 with *SD* of 0.41. Though only two variables are involved in this case, the *SD* value clearly shows the compactness of the value. Therefore, a μ value of 2.4 $\pm$0.41 served as a good PCS target safety index representative. The corresponding to the proposed target safety index is 1.44 (see Fig. 8). The resulting application of this simple mathematical expression shown in Eq. (10) will yield the PCS strength function

$$FTL = \zeta_{dl} * l_r \tag{10}$$

The ζ_{dl} symbol stands for the design load, and it is worth examining as to how this parameter relates to decking characteristics. Fig. 9 shows the relationship between ζ_{dl} and ϖ functions and shows an obvious linear relation. The projected estimation of ϖ value using the best fit shows no difference $(t = 0.04,\ dof = 11,\ p > 0.05)$. This indicates a high correlation between the pairs. Hence, the relating function between the decking characteristics and the projected design load is shown using the expression in Eq.(11).

$$\zeta_{dl} = (\varpi - 6)\ /\ 5.4 \tag{11}$$

Substitute Eq.(11) for Eq.(10), the resulting *FTL* estimate, per meter width having a span length l is

$$FTL = 0.001\zeta_{dl} f_{lr} l \tag{12}$$

The parameter f_{lr} is the load ratio factor and has a value of 1.44 from the use of the proposed PCS target safety value. Schumacher, Lääne [25] presented a similar approach that will aid in predicting PCS behavior that utilizes small-scale test with a simple model for determining the moment-curvature at critical section of a composite slab. However, in that work, the cognizance of random variability is not taken into consideration, conclusively, the new proposed FTL estimate, which takes into consideration the span length and the design load, which is dependent on sheeting deck characteristics, will give a fair estimation of the PCS load carrying capacity. By moving away from the use of awkward and expensive large-scale tests for PCS strength determination, the developed model's performance needs to be compared with the experimental test results for validation.

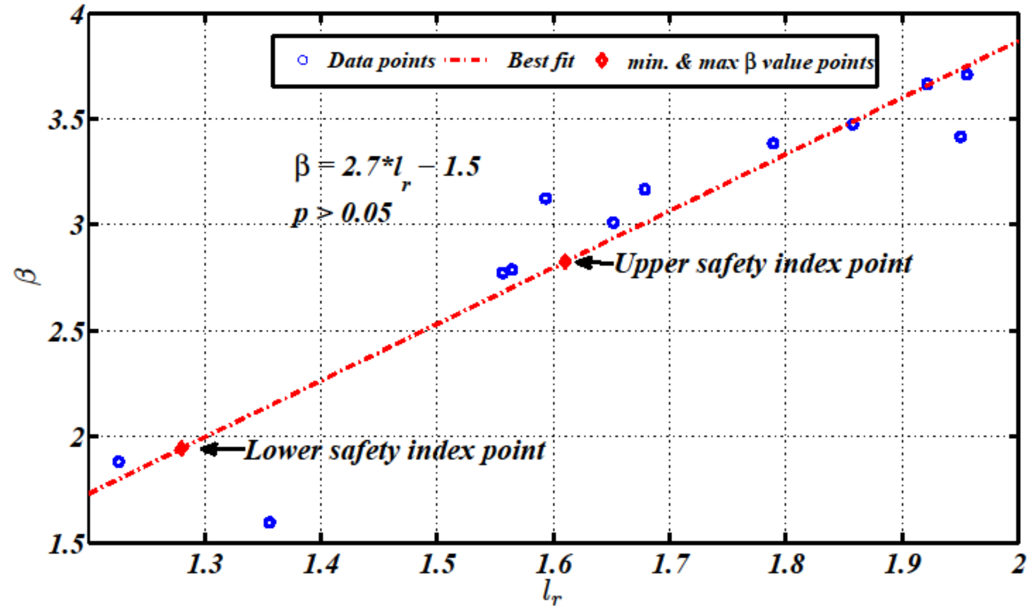

Fig. 8. Established relation between β and l_r function depicting evaluated safety index range with the use of min. and max. l_r.

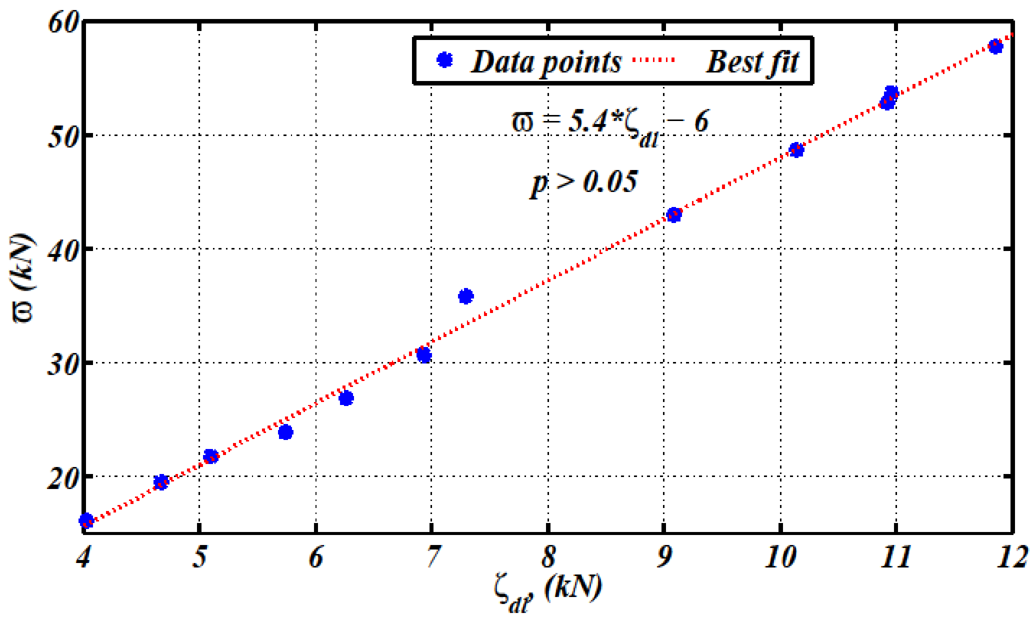

Fig. 9. An established function between design load and profiled deck characteristic.

Therefore, the following section of this paper accounts for the experimental work. This experimental result compares with the numerical function estimation in order to know the suitability of the expression shown in Eq. (12) in determining PCS failure strength.

5. Experimental test-setup

This experimental study work consists of testing of eight PCS specimens that includes two each for both long and short shear span lengths of 228 mm, 243 mm, and 305 mm, 320 mm, respectively. For simplicity, these specimens are identified using notations SS and LS; for example, SS-228 and LS-305 represent short and long specimen with a shear span length of 228 mm and 305 mm, respectively.

5.1. Materials properties and slab specimen casting

The metal deck has a thickness of about 0.47 mm, and it is 1829 mm long (L), having width (b) value of 820 mm as shown in Fig. 10. The desired concrete strength is normal grade concrete, and the mix is prepared using 20 mm aggregate for 120 mm thick concrete. For hydration control, 5.2 mm mild bars are meshed through at 220 mm both ways and placed 20 mm above the metal deck.

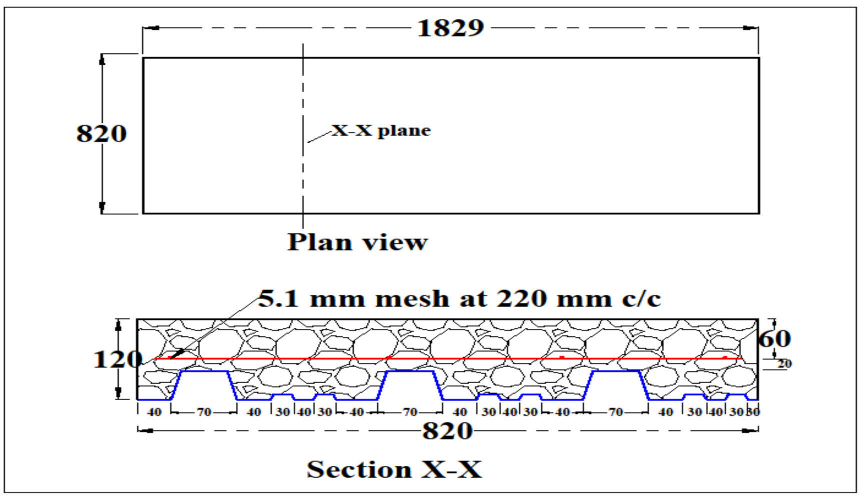

Fig. 10. Slab specimen.

All the required standard laboratory checks on the mix design prior to concreting are fully adhered to the ACI-318 standard. The concrete cubes average compressive strength is 28.55 MPa.

5.2. Experimental test set-up

Application of static load is with the use of hydraulic jack where two rollers weighing about 10 kg each are placed on top of the slab specimen with the intention of applying the two-point load from a cross beam that also weights about 70 kg. The slab overhang length l_o is 100 mm from both ends, and its failure mode is determined through an edges (decking sheet and concrete) placement of linear variable displacement transducers (LVDT) as depicted in Fig. 10. Similar LVDT's is in place at the mid-span to record the slab deflection (Fig. 12). Data logger-TDS-530 records the hysteresis history, and the testing is halted if the maximum applied load drops by about 20% or the mid-span deflection value is approaching $l/30$ [26].

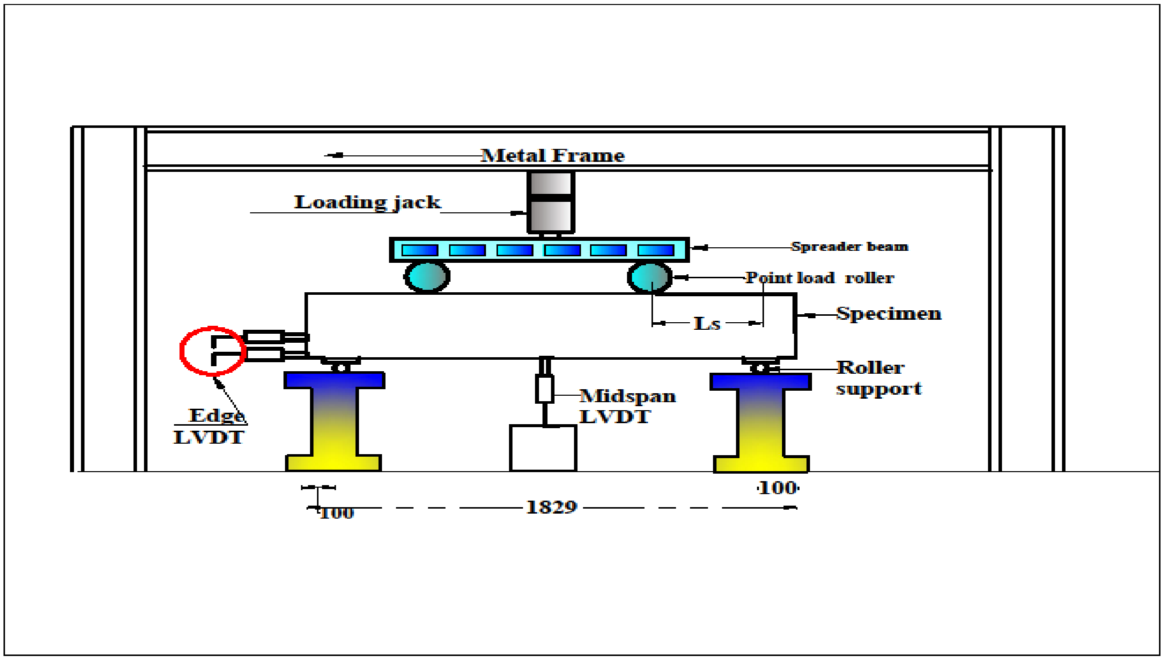

Fig. 11. Specimen experimental test set-up.

Fig. 12. LVDT arrangements.

Experimental testing results are to validate the numerical solution estimation for the strength capacity determination of PCS. The closeness between the compared results will validate the suitability of the developed model for strength capacity estimation of PCS. Hence, Fig. 13 shows the experimental performance of the tested PCS specimens. A maximum strength capacity value of 45.97 kN is recorded with the shortest shear span length, and the lengthiest shear span test value gives 27.97 kN. After the maximum peak failure load, an average of 50% unloading peak load results in a high deflection value. This explains why there is a large jump beyond the peak load value as shown in Fig. 13.

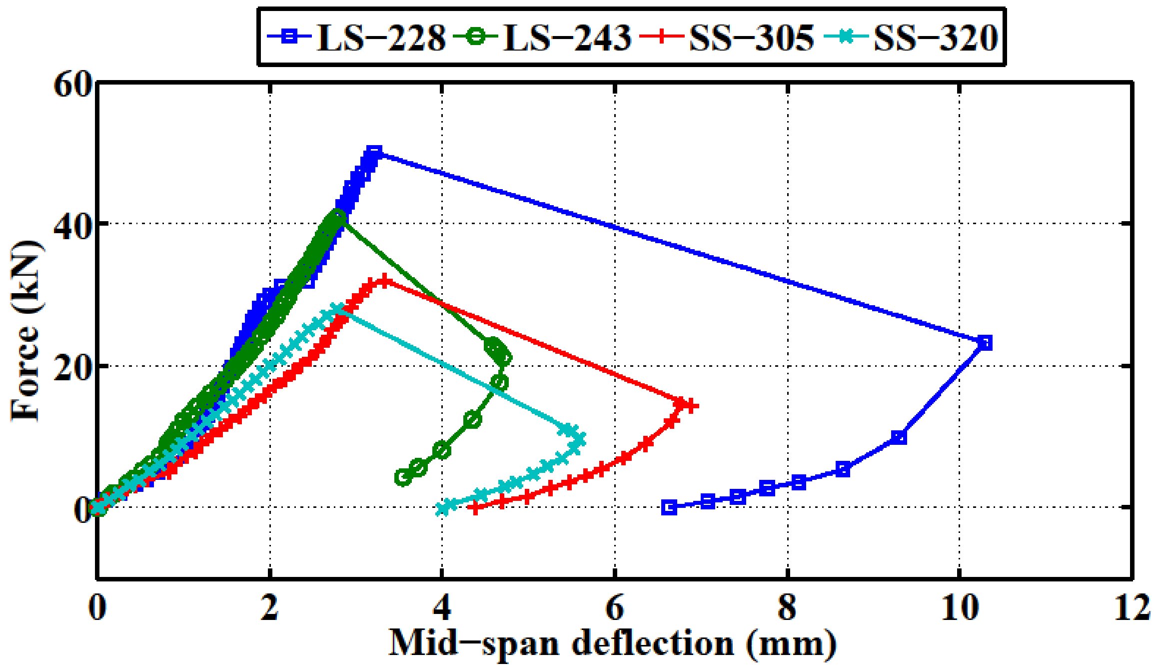

Fig. 13. Force-deflection relationships under the four shear span lengths.

6. Model verification

This paper demonstrated the application of a more rational approach to defining the safety value associated with the PCS longitudinal shear (*m-k* method). This led to the formulation of closed-form expression for the *FTL* estimate, as shown in Eq. (12). Testing the function suitability by comparative analysis with several full-scale laboratory tests value, slab test details and the experimental strength loads results together with the study's approximate strength load estimates from the use of expression in Eq. (12) are in Table 2.

Table 2 shows several PCS experiment results, and the details for the items listed can be found in the literature [4,13,22,27]. Statistically, there is no *FTL* value difference between the experimental results compared to the study's new approach in determining the *FTL* value (Table 2); Mohammed [4] ($t = 0.150,\ dof = 10,\ p \succ 0.05$),Gholamhoseini, Gilbert [13] ($t = 0.169,\ dof = 14,\ p \succ 0.05$) and this study $t = 1.490,\ dof = 6,\ p \succ 0.05$. However, the FTL values comparisons between the study's approximate estimation and the experimental result presented in Chen [22] shows a significant variance of $p \prec 0.05$ This variance is not surprising, because the resistance offered by the use of shear studs within the specimens might influence the load-bearing capacity.

Table 2
Failure test load comparative analysis.

Source	Label	A_p (mm^2)	F_{yp} (MPa)	d_p (mm)	l_s (mm)	l (m)	Experimental FTL (*kN*)	Approximate FTL (*kN*)
Gholamhoseini, Gilbert [13]	ST57-4	1434	536	135.9	850	3.4	92.8	111.34
	ST57-6	1434	536	135.9	567	3.4	154	166.95
	ST55-4	1485	534	134.6	850	3.4	67	113.7
	ST55-6	1485	534	134.6	567	3.4	102.5	170.6
	ST70-4	1320	544	122.3	775	3.1	84	96.6
	ST70-6	1320	544	122.3	517	3.1	116.5	140.35
	ST40-4	1248	475	136	775	3.1	74.4	85.92
	ST40-6	1248	475	136	517	3.1	122	128.84
Mohammed [4]	Slab 1	980	550	93	900	2.7	46.8	37.07
	Slab 2	980	550	93	900	2.7	38.1	37.07
	Slab 3	980	550	93	900	2.7	49.1	37.07
	Slab 4	980	550	93	45 0	2.7	61.9	74.2
	Slab 5	980	550	93	450	2.7	63.7	74.2
	Slab 6	980	550	93	450	2.7	65.6	74.2
Chen [22]	A-1	1170.8	380	55	650	2.6	52.7	26.04
	A-3	1170.8	380	55	800	3.2	42.8	26.02
	A-5	1170.8	380	55	650	2.6	39.8	26.04
	A-2	1561.8	380	55	650	2.6	61	37.74
	A-4	1561.8	380	55	1050	4.2	46.9	34.72
Ong and Mansurt [27]	AA1	1259	550	79	600	2.4	26	58.3
	AA2	1259	550	79	600	2.4	26	58.3
	AB1	1259	550	99	750	3	35.8	73.1
	AB2	1259	550	99	750	3	33.8	73.1
	AC1	1259	550	99	990	3	27.9	23.1
THIS STUDY EXPERIMENT	LS-228	496.7	340	100	228	1.829	45.97	35.31
	LS-243	496.7	340	100	243	1.829	41.33	33.32
	LS-305	496.7	340	100	305	1.829	33.5	26.54
	LS-320	496.7	340	100	320	1.829	27.97	25.29

The shear studs provide sustained shear capacity for a longer period even with the loss of composite action [27]. This assertion is true, because similar comparisons in *FTL* estimations from slab test specimens [27] with end anchorage show similar variance (Table 2). Rana, Uy [26] recently presented a study on the effect of end anchorage in the composite slab, and the results were those expected that shows the increase in the load carrying capacity because of the anchorage effect. This shows the mammoth contribution of shear-studs in increasing the PCS longitudinal shear capacity. However, use of such shear connectors is uneconomical, and a simple deck embossing will provide the needed degree of resistance between the decking sheet and the concrete. Hence, the study has formulated *FTL* estimate did not take in to account the shear stud influence. This limitation will definitely form the variation.

Furthermore, though the FTL comparison between the experimental and the model values shows good results considering the *p*-value function, but the load model estimation were low in some cases and vice-versa. This behavior can be attributed to the influence of the shear span length and the shear stud device used in some of the experimental tests. While the latter influence on the load model estimation was given previously, that of the shear span length on the safety performance estimation is further presented using Fig. 14 that considers the two-point load application. The analogy shows that safety value decreases with increasing shear span length towards the mid-span. This reveals the need for careful considerations for the lengthier shear span length value for experimental tests. For example in Table 2, for a span length of 2.5 m (excluding 0.2 m overhang length), the resulting use of lengthier shear span length of 900 mm results in moving the load position close to the mid-span, thus decreasing load capacity as shown with the model estimation. This behavior is similarly demonstrated experimentally where it was shown that test specimen fails to withstand the cyclic load test because of the load position close to the mid-span [16].

Fig. 15 presents the shear values comparisons amongst the experimental, theoretical and new theoretical values as a further test of the statistical significance of this new strength determination method. The experimental shear values in panels A and B are from the literature, and this study's experimental shear is under panel C. Similarly, the theoretical shears computations were obtained from the use of Eq. (4), and as are the corresponding values of the new theoretical shear from the use of approximate estimate expression with varying *FTL* estimates (10%, exact, $\pm$20%). However, in this study, the theoretical shear value could not be computed with the data from Gholamhoseini, Gilbert [13] under Fig. 15(A), because of different cross sections used in that experiment coupled with the limited sample size required for longitudinal shear value estimation.

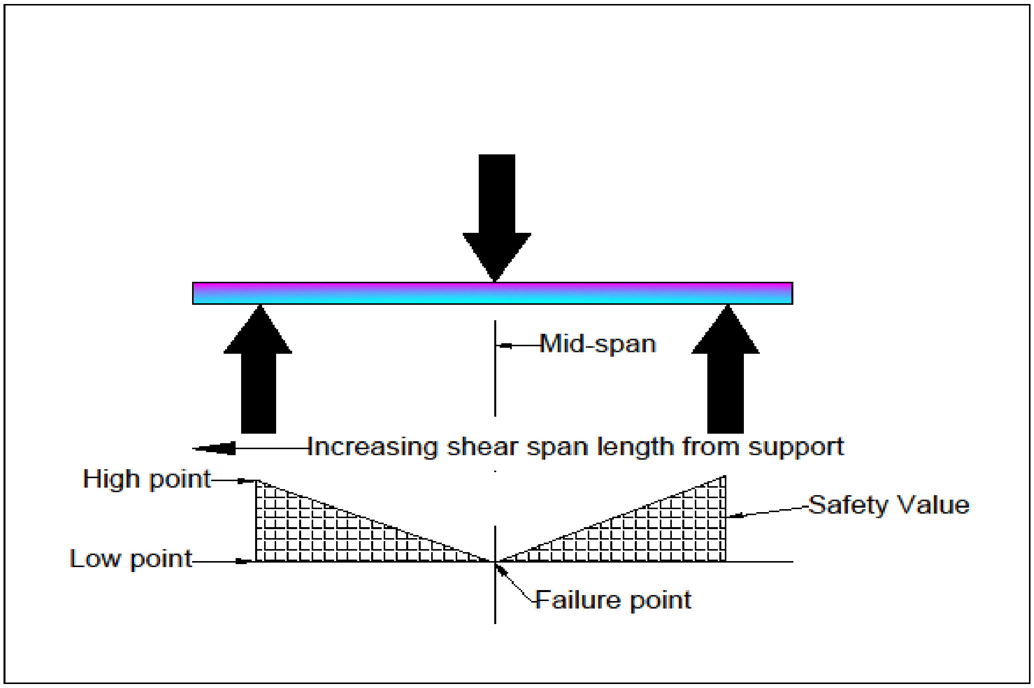

Fig. 14. Shear length influences the safety behavior of PCS.

Analytically, the results in Fig. 15 (B) and (C) show that the six shear groups differ significantly, $F(5,30) = 2.76, p \prec 0.05$ and $F(5,30) = 2.45, p \prec 0.05$ respectively, considering the shear values from the new theoretical value against the experimental and existing theoretical based computations. A similar analysis with respect to values in Fig. 15(A) with five shear groups shows a similar result, $F(4,35) = 5.03, p \prec 0.05$.

Interestingly, there is no variance between the experimental shear and the exact shear value estimates from the new theoretical relation $(t = -1.47, dof = 11, p \succ 0.05)$. A similar analysis of theoretical shear values gives a similar result with both Bonferroni corrected alpha $(t = -2.98, dof = 11, p \succ 0.05)$. These results are in agreement with previous experiments that shows the closeness between predicted shear bond strength and experimental shear value [22]. Furthermore, this is clearly validated with the experimental work where the result of numerical analysis and the experimental value shows no variations [5]. The performance of the developed model in determining PCS strength capacity is correlating well with the experimental values as expected.

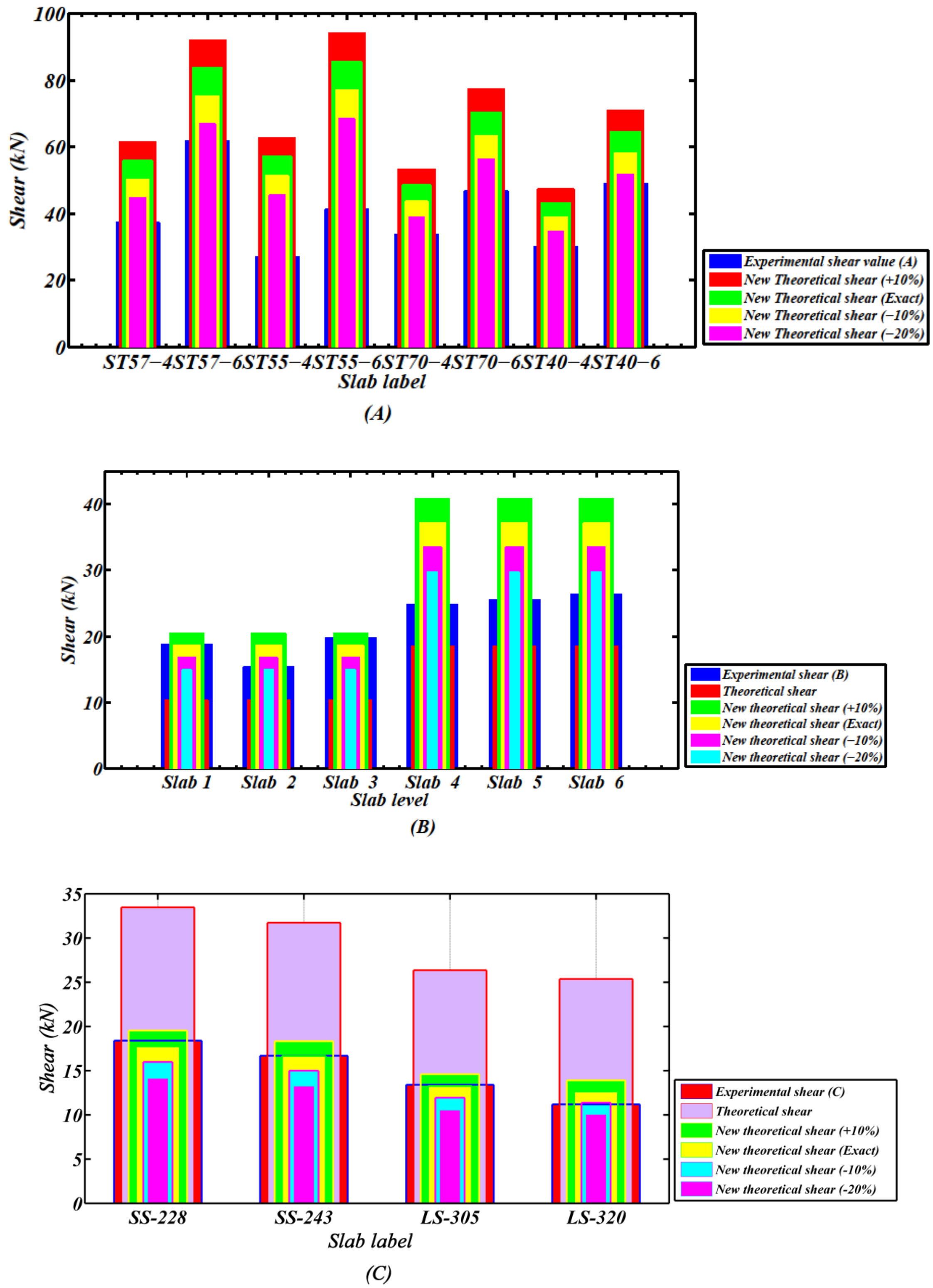

Fig. 15. Two experimental shear results in comparison with the estimate of new theoretical value. The experiment works after: (A) Gholamhoseini, Gilbert [13] (B) Mohammed [4] (C) This study experiment.

6.1. Numerical example of longitudinal shear

This section considers the numerical example of the longitudinal shear τ estimation with the use of approximate strength load for determining the *m* and *k* parameter, as shown in Table 3. The slab groups (*X* and *Y*) details and its experimental test values for this example can be found in Johnson [10]. The computed values of τ were 0.28, 0.30 and 0.24 N/mm^2, which stands as 0.27 N/mm^2 for group *X* on average. Comparatively, this study's computed value on average is 0.23 N/mm^2, which compares well with the experimental mean value result. A similar comparison shows similar results for slab group *Y*. It should be noted that these values are obtained after plotting the vertical shear against shear bond so as to obtain the *m* and *k* parameters needed for that computation.

Table 3
Longitudinal shear values example.

Group	label	A_p (mm^2)	f_{yp} (MPa)	d_p (mm)	l_s (mm)	l (m)	v (kN)	v / bd_p (N/mm^2)	A_p / bl_s
X	1-3	1543	353	132	775	3.1	30.65	0.2321	0.00199
	4-6	1543	353	112	975	3.9	25.99	0.2321	0.00158
	7-8	1543	353	102	1525	6.1	23.64	0.2319	0.00101
Y	1-3	1330	437	112	1000	4.0	27.74	0.2477	0.00133
	4-6	1330	437	112	1500	6.0	27.72	0.2475	0.00089

7. Conclusion

Despite the numerous advantages associated with the use of profiled composite slab in the construction industry, costlier and time-consuming laboratory procedures accounts for its shear characterization. Deterministically, because of the strength influencing factors, the much-needed development of a simplified strength function is hindered. This warrants this paper to develop a more simplified strength function that considers the randomness associated with those parameters. Interestingly, it is the conclusion of this paper that the suitability of the proposed target safety value and the new PCS strength determination under *m-k* method performed as expected. The litmus test comparison of load capacities (numerical and experimental) result shows promise for the numerical model in determining the strength capacity of PCS. Similarly, the behavioral shear results exhibited for the experimental and theoretical values compare well with the new theoretical estimates. Hence, this signifies the viability of this new PCS strength determination method, and this will significantly ease the high level of conservatism in characterizing PCS strength. However, the said behavior may not apply to PCS with shear transferring devices between the decking sheet and the concrete. Future studies on the development of *FTL* values by incorporating shear-transferring devices will be of great interest.

Acknowledgment

The authors will like to thank the Universiti Putra Malaysia for providing full financial support (GP-IPS/2015/9453400) required for this work.

References

[1] Karim IA, Mohammed K, Aziz NFAA, Hua LT. Comparative Safety Performance Evaluation of Profiled Deck Composite Slab from the Use of Slope-Intercept and Partial Shear Methods. World Acad Sci Eng Technol Int J Civil, Environ Struct Constr Archit Eng 2015;9:1047–53.

[2] Marčiukaitis G, Jonaitis B, Valivonis J. Analysis of deflections of composite slabs with profiled sheeting up to the ultimate moment. J Constr Steel Res 2006;62:820–30. doi:10.1016/j.jcsr.2005.11.022.

[3] Cifuentes H, Medina F. Experimental study on shear bond behavior of composite slabs according to Eurocode 4. J Constr Steel Res 2013;82:99–110. doi:10.1016/j.jcsr.2012.12.009.

[4] Mohammed BS. Structural behavior and m–k value of composite slab utilizing concrete containing crumb rubber. Constr Build Mater 2010;24:1214–21. doi:10.1016/j.conbuildmat.2009.12.018.

[5] Abdullah R, Samuel Easterling W. New evaluation and modeling procedure for horizontal shear bond in composite slabs. J Constr Steel Res 2009;65:891–9. doi:10.1016/j.jcsr.2008.10.009.

[6] Abdullah R, Hong Kueh AB, Ibrahim IS, Easterling WS. CHARACTERIZATION OF SHEAR BOND STRESS FOR DESIGN OF COMPOSITE SLABS USING AN IMPROVED PARTIAL SHEAR CONNECTION METHOD. J Civ Eng Manag 2015;21:720–32. doi:10.3846/13923730.2014.893919.

[7] An L. Load bearing capacity and behaviour of composite slabs with profiled steel sheet 1993.

[8] Crisinel M, Marimon F. A new simplified method for the design of composite slabs. J Constr Steel Res 2004;60:481–91. doi:10.1016/S0143-974X(03)00125-1.

[9] Degtyarev V V. Reliability-Based Evaluation of U.S. Design Provisions for Composite Steel Deck in Construction Stage. J Struct Eng 2012;138:308–17. doi:10.1061/(ASCE)ST.1943-

541X.0000437.

[10] Johnson RP. Models for the Longitudinal Shear Resistance of Composite Slabs, and the Use of Non-Standard Test Data. Compos Constr Steel Concr V, Reston, VA: American Society of Civil Engineers; 2006, p. 157–65. doi:10.1061/40826(186)16.

[11] Johnson RP. Composite structures of steel and concrete: beams, slabs, columns, and frames for buildings. John Wiley & Sons; 2008.

[12] BEng SH, Park S. EN 1994-Eurocode 4: Design of composite steel and concrete structures n.d.

[13] Gholamhoseini A, Gilbert RI, Bradford MA, Chang ZT. Longitudinal shear stress and bond–slip relationships in composite concrete slabs. Eng Struct 2014;69:37–48. doi:10.1016/j.engstruct.2014.03.008.

[14] Marimuthu V, Seetharaman S, Arul Jayachandran S, Chellappan A, Bandyopadhyay TK, Dutta D. Experimental studies on composite deck slabs to determine the shear-bond characteristic values of the embossed profiled sheet. J Constr Steel Res 2007;63:791–803. doi:10.1016/j.jcsr.2006.07.009.

[15] Holmes N, Dunne K, O'Donnell J. Longitudinal shear resistance of composite slabs containing crumb rubber in concrete toppings. Constr Build Mater 2014;55:365–78. doi:10.1016/j.conbuildmat.2014.01.046.

[16] Hedaoo N, Gupta L, Ronghe G. Design of composite slabs with profiled steel decking: a comparison between experimental and analytical studies. Int J Adv Struct Eng 2012;4:1. doi:10.1186/2008-6695-3-1.

[17] EC4 E in D of composite steel and concrete structures. Part1.1: General rules and rules for building (PrEN 1994-1-1:2003) 2003.

[18] Okasha NM, Aichouni M. Proposed Structural Reliability-Based Approach for the Classification of Concrete Quality. J Mater Civ Eng 2015;27:04014169. doi:10.1061/(ASCE)MT.1943-5533.0001131.

[19] Robert EM. Structural reliability analysis and prediction. Baffins Lane, Chichester, West Sussex, Engl Wiley 1999.

[20] Adrzej SN, Anna MR, Ewa KS. Revised statistical resistance model for reinforced concrete structural component. ACI 2012;284:1–16.

[21] Ellingwood B, Galambos T V. Probability-based criteria for structural design. Struct Saf 1982;1:15–26. doi:10.1016/0167-4730(82)90012-1.

[22] Chen S. Load carrying capacity of composite slabs with various end constraints. J Constr Steel Res 2003;59:385–403. doi:10.1016/S0143-974X(02)00034-2.

[23] Abdinasir Y, Abdullah R, Mustaffa M. Modelling of shear bond with cohesive element and slenderness study of composite slabs. Proc Jt Conf 8th Asia Pacific Struct Eng Constr Conf 1st Int Conf Civ Eng Conf (ICCER), APSEC-ICCER 2012, 2012, p. 2–4.

[24] Honfi D, Mårtensson A, Thelandersson S. Reliability of beams according to Eurocodes in serviceability limit state. Eng Struct 2012;35:48–54. doi:10.1016/j.engstruct.2011.11.003.

[25] Schumacher A, Lääne A, Crisinel M. Development of a New Design Approach for Composite

Slabs. Compos Constr Steel Concr IV, Reston, VA: American Society of Civil Engineers; 2002, p. 322–33. doi:10.1061/40616(281)28.

[26] Rana MM, Uy B, Mirza O. Experimental and numerical study of end anchorage in composite slabs. J Constr Steel Res 2015;115:372–86. doi:10.1016/j.jcsr.2015.08.039.

[27] Ong KCG, Mansurt MA. Shear-bond capacity of composite slabs made with profiled sheeting. Int J Cem Compos Light Concr 1986;8:231–7. doi:10.1016/0262-5075(86)90050-3.